Top Organomet Chem (2023) 70: 67–98
https://doi.org/10.1007/3418_2022_79

Published online: 3 January 2023

Chemical Transformations in Heterobimetallic Complexes Facilitated by the Second Coordination Sphere

R. Malcolm Charles III and Timothy P. Brewster

Contents

Abstract This chapter is dedicated to heterobimetallic complexes in which the two metal centers are not directly bound. Complexes are described in which the second metal resides in the second coordination sphere of the first metal and enables bond activation processes via synergistic activity with the first metal that are not available to the corresponding monometallic complexes. Both stoichiometric and catalytic bond activations are analyzed in the light of the type of reactions (e.g., H_2 activation, polymerization, etc.). Both steric and electronic effects appear to play significant roles in many cases, and as such, they are examined when applicable. Indeed, spatial proximity between the two metal centers as well as electronic environment can allow for modification and tuning of reactivity. This realization has led to the development of switchable catalytic systems which are highlighted and discussed in terms of how they are manipulated (e.g., redox-switchable systems and cation-responsive systems). While significant progress has been made toward furthering our collective understanding of the behavior of these types of heterobimetallic complexes, this area

R. Malcolm Charles III
Department of Chemistry, The University of Memphis, Memphis, TN, USA
e-mail: rmchrles@memphis.edu

T. P. Brewster (✉)
Department of Chemistry, Faculty of Chemistry, The University of Memphis, Memphis, TN, USA
e-mail: tbrwster@memphis.edu

is still ripe for future development. Additional systematic work is necessary to continue to push this area of chemistry forward.

Keywords Bimetallic · Bond activation · Catalysis · Heterobimetallic · Migratory insertion · Oxidative addition · Reactivity · Reductive elimination · Second coordination sphere

1 Introduction

As the field of bimetallic chemistry continues to develop, it can be beneficial to separate bimetallic structures into two structural categories. In the first category the two metals are covalently bound to each other. Positioning a second metal in the primary coordination sphere of a metal center allows for strong electronic modulation and positions the system for cooperative bond-breaking events. Structures of this type have been widely explored and feature in a number of review articles as well as other chapters within this volume [1–5].

The second category of complex contains bimetallic structures in which the two metal centers are not bound to each other, *but rather exert second coordination sphere effects on each other*. Electronic influence between the two sites is weaker than in directly bound systems, which allows the two metal centers to operate with more independence and to retain properties that these metals would be likely to exhibit in monomeric complexes. However, being tied together in a bimetallic construct can help to overcome kinetic and/or stability issues that can arise in tandem catalytic systems.

Our chapter focuses on this second class of bimetallic complex, with a particular focus on complexes that have been structurally characterized. As an introduction, we will first discuss representative applications of such complexes in stoichiometric bond activations, then move on to explore select, instructive catalytic applications, before finally discussing an emerging area of research in which one metal center is used to switchably attenuate the reactivity at the second metal site. While not designed as an exhaustive literature review of bond activation or catalysis mediated by bimetallic complexes (this has been done elsewhere) [2, 6–8], this chapter will provide a tutorial review sampling the breadth of reactivity that is available in second-sphere systems.

2 Stoichiometric Bond Activation Mediated by the Second Coordination Sphere

Second coordination sphere effects manifest in a number of different ways. The section below will highlight examples that are both unique and instructive. When considering stoichiometric bond activations in bimetallic systems, it is important to distinguish between systems in which the two metal centers act cooperatively and systems in which the two metal centers function somewhat independently. We will consider as "cooperative" bond activations those in which both metal centers are (or likely are) active participants in the elementary step during which the key bond-breaking event occurs. Other systems, where a single metal center is responsible for bond breaking and the second metal serves a separate function (electronic modifier, steric blocking, etc.), will be considered as non-cooperative. Both motifs are frequently encountered.

Our first instructive example, a heterobimetallic potassium-aluminum dimer that, remarkably, functions as a nucleophile, falls into the non-cooperative category (Scheme 1) [9]. In this system the presence of the potassium cation stabilizes a formally Al(I) center bearing a nucleophilic lone pair. The cation is not directly bound to the aluminum center, but rather interacts with aromatic substituents on the sterically bulky pincer ligand employed. Only a strongly electropositive, reducing metal center would be able to stabilize an Al(I) aluminyl in a bimetallic construct. The nucleophilic K-Al heterobimetallic construct was found to activate H_2 and oxidatively add benzene via C–H bond activation. This study represents the first example of intermolecular oxidative addition of a C–H bond in benzene at a single, well-defined, main-group metal center (Scheme 2), with reactivity made possible by the outer-sphere stabilization imparted by the potassium cation.

In a mechanistically similar example, hydrogen activation by heterobimetallic iridium-aluminum and rhodium-aluminum complexes was reported, as shown in Scheme 3 [10]. This system is comprised of a late transition metal center bound to a second-sphere aluminum functionality. In the solid state the two metal centers are separated by over 4 Angstroms preventing the formation of a direct metal–metal bond [11]. Despite the long internuclear distance and relatively weak electronic effect the aluminum site exerts on the transition metal, the system is still able to achieve reactivity that the late transition metal center could not achieve

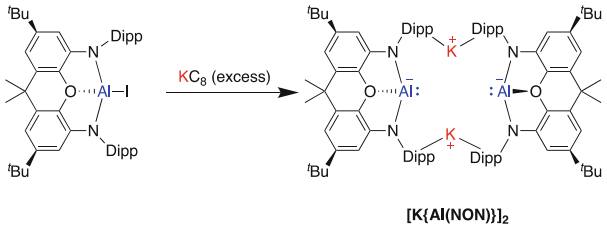

Scheme 1 Synthesis of K-Al heterobimetallic dimer

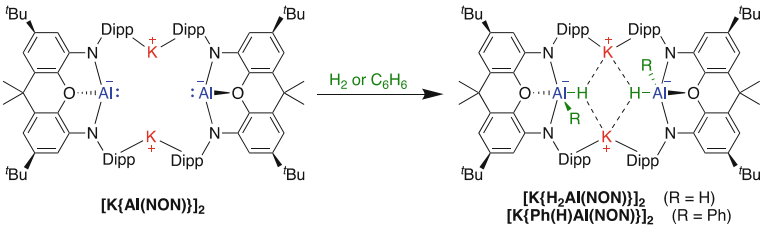

Scheme 2 H_2 activation and oxidative addition of benzene by K-Al heterobimetallic

Scheme 3 General H_2 activation and hydrogenolysis reaction

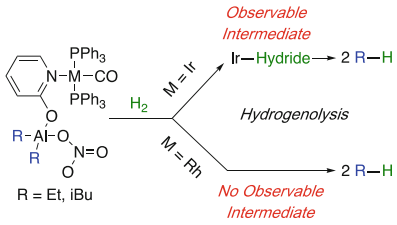

independently. Both Ir and Rh were found to react with hydrogen to generate the observed final product of alkane gas.

A series of kinetic experiments were undertaken to distinguish between several possible, plausible reaction mechanisms (Scheme 4). The authors determined proposed mechanism 1 to be the most likely reaction mechanism, based on derivation of a second-order rate and, in the case of Ir, observation of a stable intermediate resulting from oxidative addition of hydrogen to the transition metal. The transition metal facilitates a classical oxidative addition reaction and subsequently transfers hydrides to the aluminum alkyls, functioning as acceptors, in the second coordination sphere. Notably, while 16-electron Ir centers are well known to oxidatively add H_2, the corresponding oxidative addition reaction with the utilized Rh complexes is endergonic. The reaction proceeds only because the strongly basic aluminum alkyls provide a thermodynamic driving force. The overall mechanics of this stoichiometric reactivity are akin to a tandem catalytic process.

The remaining examples discussed in this section focus on cooperative reactivity. In cooperative second-sphere reactions the two metal centers can function in a manner similar to a Frustrated Lewis Pair (FLP) [12–17], such that they can be considered "masked FLPs." The result is a heterolytic bond cleavage. A beautiful example of this concept is a platinum-aluminum heterobimetallic complex, synthesized in 2016. The Z-type complex was shown to sequester CO_2, CS_2, and to stoichiometrically activate molecular hydrogen via oxidative addition of H–H bonds at elevated temperature (80°C) and pressure (3 bar) (Scheme 5) [18].

At first glance, this reaction may not appear to be a second-sphere process. However, DFT calculations revealed that each step in the reaction is facilitated by

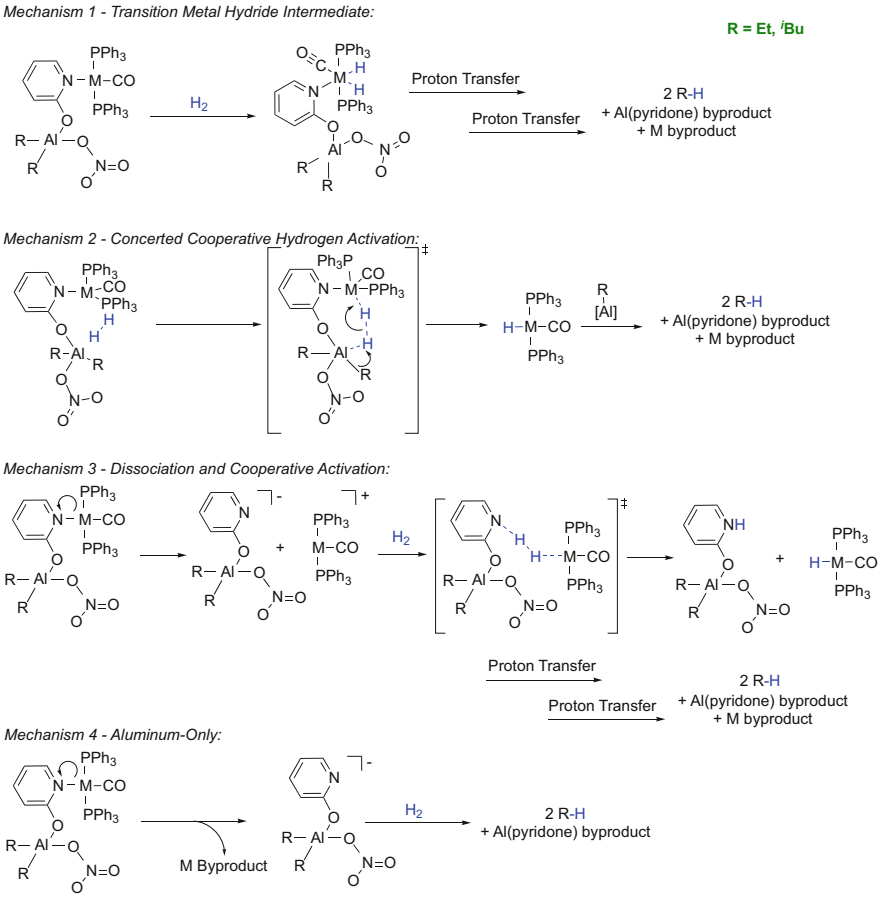

Scheme 4 Considered reaction mechanisms for the reaction of Rh/Ir-Al heterobimetallics with hydrogen

Scheme 5 Hydrogen activation by Pt-Al heterobimetallic

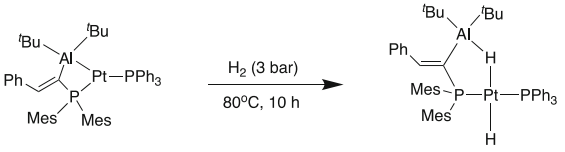

stabilizing interactions with the Al moiety; thus, cooperative interaction between the two metal centers is required for successful H_2 activation. Indeed, the formal Z-type bond between the Pt center and Al is cleaved first, followed by subsequent H_2 coordination. This results in a bridged dihydrogen complex, making this a true second-sphere effect.

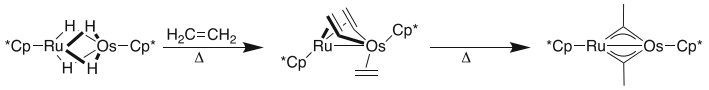

Scheme 6 Reaction of Ru-Os heterobimetallic with ethylene

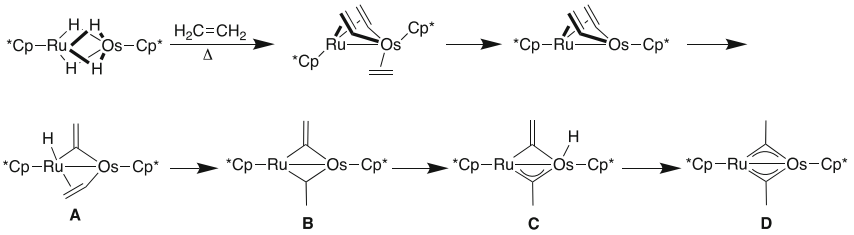

Scheme 7 Proposed mechanism for reaction of Ru-Os heterobimetallic with ethylene

The examples described above beautifully illustrate how a second metal in the second coordination sphere can modulate reactivity. In the first example, the aluminum center is able to access a reactivity manifold (oxidative addition) that is otherwise very unlikely to occur due to the instability of Al(I) complexes. In the second, a tandem-like system is generated in which each metal undergoes a more "standard" reactivity pattern. Finally, our third example demonstrates cooperative bond activation. The final highlighted examples of stoichiometric reactivity that we will present illustrate a different type of cooperative reactivity. As a direct contrast to this system, two metal centers which are initially separated by a bridging ligand are found to be directly bound in the final product.

An Ru-Os tetrahydrido heterobimetallic complex that reacts with ethylene to exclusively generate a divinyl-ethylene complex is shown in Scheme 6 [19]. This report is reminiscent of earlier work from the authors on a related Ru-Ru homobimetallic system [20–22].

The authors proposed a mechanism for this reaction (Scheme 7) in which emancipation of the coordinated η [2]-ethylene, followed by oxidative addition of the C(α) − H bond of one of the two vinyl groups at Ru, produces μ-vinylidene species **A**. **A** then undergoes insertion of the remaining vinyl group into an Ru − H bond giving μ-ethylidene-μ-vinylidene intermediate **B**. Subsequent α-H elimination from the μ-ethylidene ligand followed by insertion of the μ-vinylidene moiety into an Os−H bond would afford the final bis-ethylidyne product **D**, via intermediary μ-vinylidene-μ-ethylidyne complex **C**. This report represents the first example of a heterobimetallic tetrahydrido-bridged complex having neither phosphine nor carbonyl ligands, and the heterobimetallic product **D** contains a newly formed M-M bond between Ru and Os.

This work was extended further with the advent of an Ir-Zr heterobimetallic complex bridged by hydrides (Scheme 8) [23]. These heterobimetallics, the authors demonstrated, were able to facilitate H/D exchange reactions between C_6D_6 and

Scheme 8 Ir-Zr heterobimetallic complex

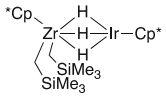

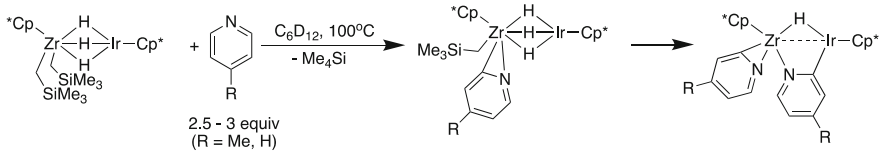

Scheme 9 Reaction of Ir-Zr heterobimetallic with pyridine derivatives

methoxyarenes as well as C–H activation of pyridine derivatives. Interestingly, as with their previously mentioned Ru-Os report [19], the heterobimetallic product resulting from the pyridine C–H activation reactions contains a newly formed bond between the Zr and Ir metal centers (Scheme 9).

3 Catalysis Mediated by the Second Coordination Sphere

The general reaction motifs encountered above can be extended into catalytic applications. In each of the catalytic reactions discussed below, the role of the "secondary" metal in modulating the reactivity of the "primary" catalytic metal will be presented in the context of the stoichiometric reactions above.

A common application of bimetallic complexes in catalysis is polymerization [24–35]. The prevalence of metallocene and other homogeneous transition metal olefin polymerization catalysts that are activated by methylalumoxane (MAO) has historically been a significant driver for this work. With the goal of removing the stoichiometric (or often superstoichiometric) MAO activator from the system, homogeneous polymerization catalysts tethered to Lewis Acid activators have been sought after for some time. In many cases, the Lewis Acid activator (typically aluminum) is directly bound to the early metal center [36–39]. The examples presented here extend beyond simple catalyst activation protocols. These systems contain two potentially active catalyst sites in constrained environments. The result is a synergistic effect akin to the second stoichiometric example above: each metal is performing a task it is known to achieve in monometallic systems, but the *overall processes,* in these cases the properties of the obtained polymers, are enforced by the bimetallic construct.

In 2004, a Ti-Zr heterobimetallic complex was synthesized and its ability to catalyze ethylene polymerization was demonstrated (Scheme 10) [40]. The heterobimetallic catalyst is highly active for the generation of high-molecular-weight, long-chain branched polyethylene. In contrast, control experiments

Scheme 10 Heterobimetallic Ti-Zr catalyst for ethylene polymerization

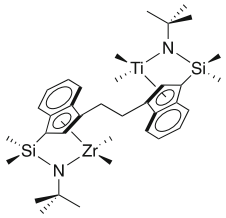

Scheme 11 Ti-W olefin polymerization catalyst

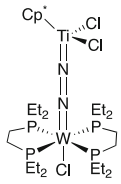

Scheme 12 Ti-Cr ethylene polymerization catalysts

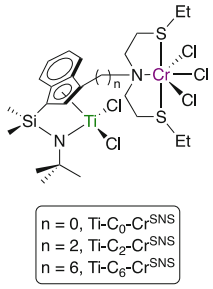

involving mixtures of monomolecular Ti and Zr complexes generate polymeric products with negligible branching. The authors attributed this to the covalent linkage between the two transition metal centers. Due to the covalent linkage, the two metals are sterically constrained such that the oligomer/macromonomer capture/enchainment is significantly enhanced.

Around the same time, a Ti-W heterobimetallic was reported that functions as a catalyst for olefin polymerization (Scheme 11) [41]. The Ti-W catalyst exhibited a remarkably high activity for the copolymerization of 1-hexene and ethylene of 510 kg mmol(cat)$^{-1}$ h^{-1}. In fact, even at reaction temperatures as high as 150°C, the catalyst was highly active for several minutes. Also, the Ti-W heterobimetallic was found to be a more active ethylene homopolymerization catalyst than a structurally similar constrained geometry catalyst (CGC).

More recently, in 2014, a series of three Ti-C_n-Cr heterobimetallic complexes were found to catalyze ethylene polymerization (Scheme 12) [42]. All three catalysts afford linear low-density polyethylenes (LLDPEs) containing exclusive *n*-butyl branches under identical conditions. The Ti-C_0-Cr^{SNS} catalyst is more active and yields polyethylenes with higher branch density than the Ti-C_2-Cr^{SNS} and Ti-C_6-Cr^{SNS}. Moreover, the authors performed additional studies which further indicate

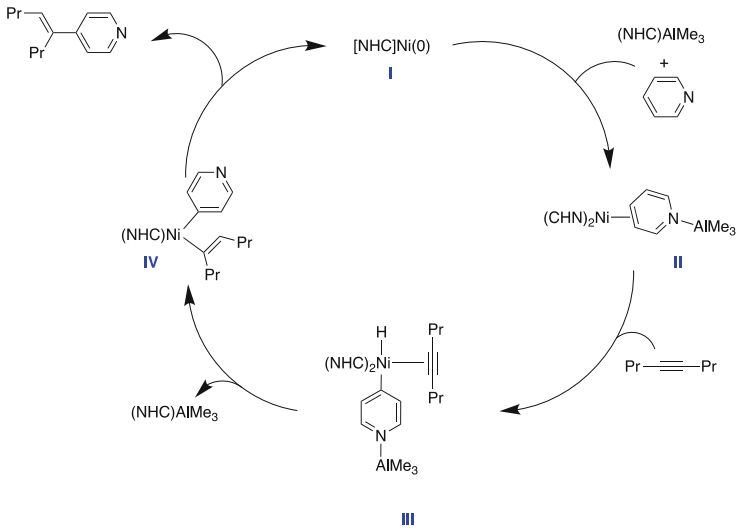

Scheme 13 Proposed catalytic cycle for *p*-selective pyridine alkenylation

that decreased spatial proximity between the two metal centers results in lower catalytic activity. That is, the further away the two metals are from each other (the longer the bridging carbon chain, C_n), the less catalytically active the heterobimetallic complex, which the authors attributed to diminished chain transfer rates.

Second-sphere effects are not limited to polymerization reactions. Applications in C-H functionalization have also been explored. The ability of one metal to *sterically direct* reactivity in such systems is a promising avenue that is now beginning to bear fruit.

A Ni-Al heterobimetallic was developed that catalyzed *para*-selective alkenylation of pyridine [43]. The authors described a possible catalytic cycle (Scheme 13). Heterobimetallic complex **II** is generated via addition of pyridine and (NHC)$AlMe_3$ (NHC = N-heterocyclic carbene) to (NHC)Ni (**I**). Ni-H intermediate **III** is then produced by oxidative addition of the alkyne to **II**. Subsequent alkyne insertion into the Ni-H bond yields **IV**. Subsequent reductive elimination yields alkenylated product and regenerates **I**. Of note, proposed Ni-Al intermediate **II** proved to be isolable and structurally characterizable, thereby serving as the first structurally isolated example of C–H activation via a synergistic effect resulting from a Ni–Al interaction.

Direct C-4-selective pyridine alkylation catalyzed by a Ni-Al heterobimetallic was reported around the same time. Furthermore, in their report, a plausible catalytic cycle similar to that described above (Scheme 13) was proposed as well (Scheme 14) [44]. The aluminum center is determined to activate the pyridine ring and to sterically compel reactivity at the electronically activated *para* position. Oxidative

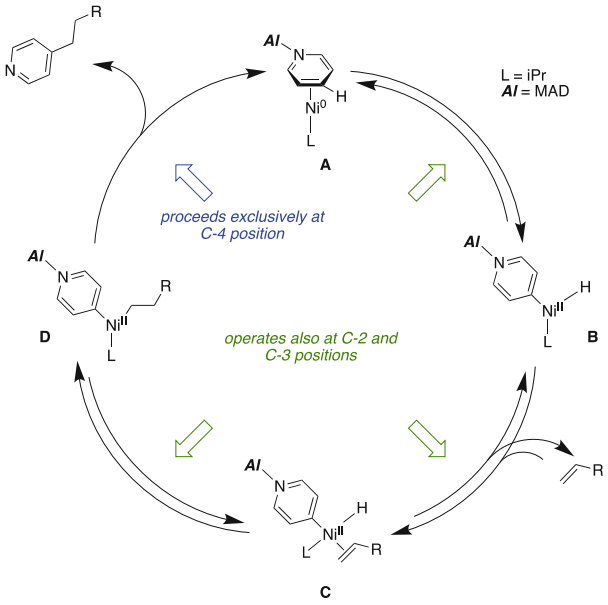

Scheme 14 Proposed catalytic cycle for C-4-selective alkylation of pyridine catalyzed by Ni-Al heterobimetallic

addition of the pyridine C(4)-H bond of **A** affords **B**. Subsequent alkene coordination yields **C**, which then undergoes migratory alkene insertion into the Ni-H bond to give **D**. Finally, reductive elimination releases C-4-alkylated pyridine and regenerates **A**. The bulky NHC ligands and (2,6-*t*-Bu_2-4-Me-$C_6H_2O)_2$AlMe (MAD) were found to be critical for promoting C-4 selectivity in both the oxidative addition and reductive elimination steps. This represents the first example of direct C-4-selective alkylation of pyridines by a Ni-Al catalyst.

The ability of a Ni-Al heterobimetallic to catalyze dehydrogenative [4 + 2] cycloaddition of formamides with alkynes has been investigated and an accompanying catalytic cycle was proposed (Scheme 15) [45].

The proposed catalytic cycle begins with η^2 coordination of Al-bound formamide to Ni, affording **A**, which then oxidatively adds the formyl C–H bond to generate **B**. Alkyne coordination followed by migratory insertion yields **C** and **D**, respectively. A second C–H activation via concerted cyclometalation results in **E**. This is followed by a second migratory insertion of a coordinating alkyne to give **F**. Subsequent reductive elimination of the $AlMe_3$-containing cycloadduct follows. Finally, decomplexation of $AlMe_3$ from the cycloadduct-generated product followed by recomplexation of $AlMe_3$ with another molecule of formamide enables regeneration of **A** via η^2 coordination.

The ability of a Ni-Al heterobimetallic to promote regioselective C–H activation of benzimidazole has also been discovered [46]. The heterobimetallic structure produces a steric restriction for the realization of the linear insertion product of

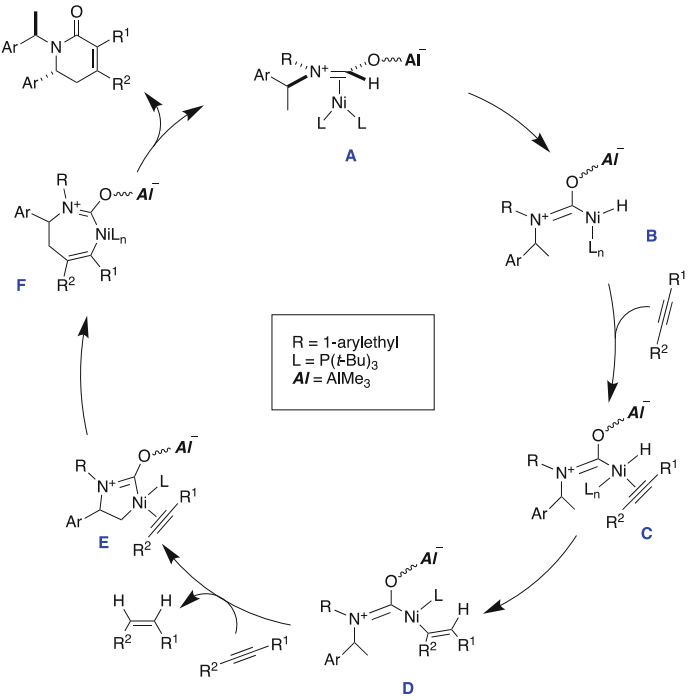

Scheme 15 Proposed catalytic cycle for dehydrogenative [4 + 2] cycloaddition of formamides with alkynes

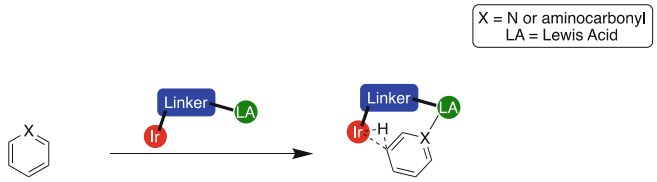

Scheme 16 Overall reaction scheme for *m*-selective C–H borylation of benzamides and pyridines

benzimidazole into styrene, while the employment of monometallic $Ni(COD)_2$ as the catalyst generates a change in favor of the branched product.

More recently, an Ir-Al heterobimetallic was described that catalyzes *meta*-selective benzamide and pyridine C–H borylation [47]. Various functional groups – N-containing, O-containing, amine, ether, and carbonyl functionalities – were well tolerated without experiencing a decline in selectivity, yielding the respective functionalized pyridylborates. Significantly, this report highlights the potential of Lewis acid–base interactions to serve as powerful instruments for manipulating site-selectivities of catalytic C–H functionalization reactions at remote positions (Scheme 16).

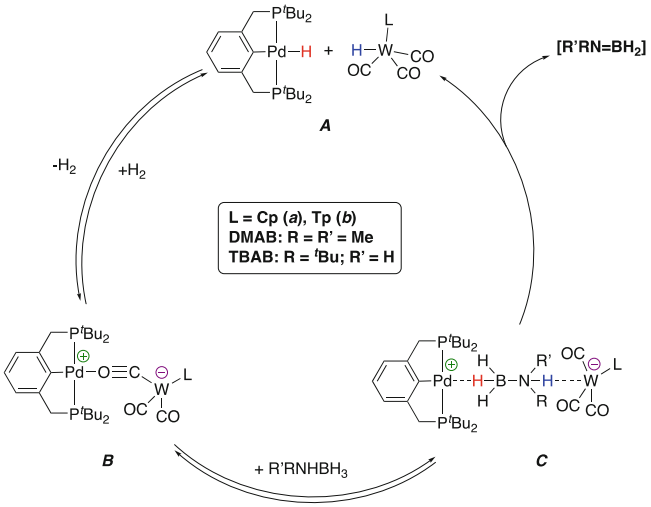

Scheme 17 Proposed catalytic cycle for amine-borane dehydrogenation by W-Pd heterobimetallic

Scheme 18 Ir-Os heterobimetallic catalyst for acceptorless and base-free dehydrogenation of secondary alcohols

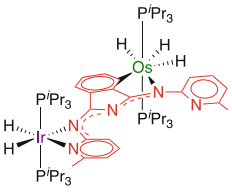

The next catalytic example presented in this section features a cooperative bond-breaking step. Similar to the example above (Scheme 5), each metal is involved in substrate activation in a manner akin to a Frustrated Lewis Pair (FLP). A W-Pd heterobimetallic complex was reported that catalyzes the dehydrogenation of amine-borane. The authors were able to propose a plausible catalytic cycle (Scheme 17) [48]. First, independent monometallic Pd-hydride and W-hydride complexes, collectively labeled **A**, react with each other to release H_2 and generate heterobimetallic complex **B**. Then, the amine-borane substrate inserts into **B** to generate **C**. Subsequent proton transfer from NH to W and hydride transfer from the BH group to Pd results in elimination of the $BH_2 = NMe_2$ product and the formation of bimetallic hydride species **C**. Finally, **C** ejects H_2 to yield **A** which interacts again to regenerate catalytically active heterobimetallic complex **B**.

In 2020, an Ir-Os heterobimetallic complex was described that catalyzes the acceptorless and base-free dehydrogenation of secondary alcohols (Scheme 18) [49]. During the course of their investigation, the authors synthesized monometallic and homobimetallic Ir analogues. Interestingly, these analogues also serve as catalysts for acceptorless and base-free secondary alcohol dehydrogenation, yet the homobimetallic is more efficient than the monometallic, and the heterobimetallic

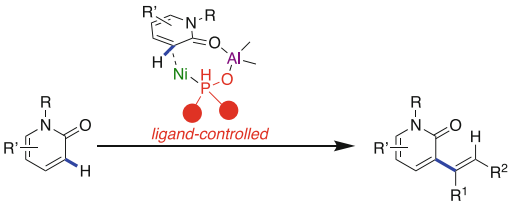

Scheme 19 General 2-pyridone C_3–H alkenylation reaction catalyzed by Ni-Al heterobimetallic

Ir-Os catalyst is more efficient than the homo- and monometallic analogues (i.e., Ir-Os > Ir-Ir > Ir).

The superior efficiency of the heterobimetallic catalyst compared to the other analogues is attributed by the authors, and we believe correctly so, to the synergistic behavior between the two different metal sites. Indeed, as mentioned before, this type of increased efficiency, along with new modes of reactivity, is a major driving force behind the interest in heterobimetallic research overall.

Recently, a Ni-Al heterobimetallic was reported to catalyze C_3–H alkenylation of 2-pyridones with alkynes (Scheme 19) [50].

A series of control experiments were performed which reinforced the importance of the PO ligand bound heterobimetallic catalyst to reaction success, as the reaction did not proceed in the absence of Ni, Al, or PO ligand. Furthermore, it was determined that the structure of the PO itself also had a profound impact on the reactivity, which is not without precedent [51]. The PO ligand needed to be sterically bulky enough to promote C–H cleavage by forcing the Ni center to approach the reaction site more closely. This is yet another fine example of how sterics should always be contemplated when considering possible reactivities and designing potential catalysts.

The breadth of potential catalytic reactivity in second-sphere bimetallic systems is immense. Reactivity patterns and motifs which have been discovered in stoichiometric reactions have been found to translate directly into catalytic systems. With the field in its relative infancy, there is a huge amount of space for future development in the coming years.

3.1 Switchable Systems

We finally turn our attention to an emergent area of research, switchable catalysis. Bimetallic systems are ideal for switchable systems. With highly differentiated metal centers, one can predictably change the structure (coordination sphere, oxidation state, etc.) at one metal center selectively. The structural or electronic change at this second-sphere metal center is "felt" by the catalytically active metal site. If the felt change is large enough, the catalyst can be turned on and off, or the nature of the obtained catalysis product can be altered. Potential applications for this technology are vast. In this last section we will give a brief overview of two forms of second-

sphere catalyst switching: redox-switchable catalysts and cation-responsive catalysts.

3.1.1 Redox-Switchable Systems

The reader will notice that ferrocene and cobaltocene are overwhelmingly utilized as the "switch" in ligand-based redox-switchable systems. This is due to the fact that they are both redox-active moieties at moderate electrochemical potentials so their electronics can be readily tuned without interference from the catalytically active site. Their redox changes are also highly reversible (ferrocene is a normal electrochemistry standard). Finally, they are substitutionally inert [52]. That is to say, upon changing their electronics, the metallocene remains attached to the scaffold containing the second metal in the bimetallic system. All of these properties, when combined make them ideal choices for a redox switch.

In 1995, a seminal study in the field of redox-switchable catalysis utilizing a metallocene switch was published [53]. In their investigation, the authors showed that an Rh-Co heterobimetallic containing cobaltocene in its reduced form $[Rh\text{-}Co]^{red}$ was a better olefin hydrogenation catalyst than its oxidized analogue $[Rh\text{-}Co]^{ox}$ (Scheme 20). In contrast, they found the opposite to be true in the case of acetone hydrosilylation, in which case $[Rh\text{-}Co]^{ox}$ was a superior catalyst than $[Rh\text{-}Co]^{red}$. The authors attributed the differences in catalytic activity to multiple possibilities, including difference in electron "donicity" as well as phosphine basicity, both of which have literature precedent [54–59].

Extension of redox-switchable behavior to olefin metathesis has been achieved. Redox switching can control the reactivity of a Grubbs–Hoveyda-type olefin metathesis catalyst that has been tagged with redox-active ferrocene (Scheme 21) [60]. Interestingly, the authors were able to use the redox-active ferrocene moieties not only to switch catalytic activity for Ring-Closing Metathesis (RCM) of *N*-tosyldiallylamide on and off, but also to control the solubility of the catalyst. By oxidizing the ferrocenyl tags, the resulting inactive dicationic catalyst precipitates out within seconds, allowing for the product to be easily separated by filtration. The

Scheme 20 Rh-Co olefin hydrogenation and acetone hydrosilylation catalysts (oxidized, red; reduced, green)

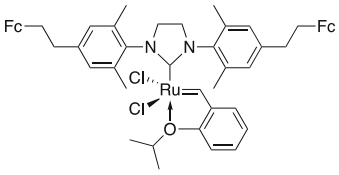

Scheme 21 Ferrocene-tagged redox-switchable Grubbs–Hoveyda type olefin metathesis catalyst

Scheme 22 Redox-switchable heterobimetallic Ru-Fe catalyst for ring-closing metathesis

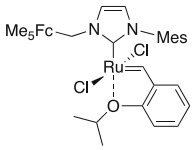

Scheme 23 Redox-switchable Ru-Fe ring-opening metathesis polymerization catalyst

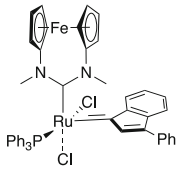

catalyst can then be switched back on via reduction, allowing for easy catalyst recycling.

Building upon this report, in 2013 an Ru-Fe heterobimetallic was prepared that served as a redox-switchable catalyst for RCM of diethyl diallylmalonate (Scheme 22) [61].

The authors showed that oxidation of the catalyst caused a dramatic decrease in catalytic activity, presumably due to reduced electron density at the metal center. Subsequent reduction with decamethylferrocene resulted in a greater than 94% return to initial catalytic activity. Thus, following one full redox cycle, the catalyst still functions at greater than 94% of its original catalytic activity. Also significant, this work represents the first example of a homogeneous, redox-switchable, NHC-supported Ru catalyst used to control RCM via modification of ligand electronics.

Around the same time, a different redox-switchable Ru-Fe heterobimetallic complex was reported that catalyzed the RCM of diethyl diallylmalonate as well as the ring-opening metathesis polymerization (ROMP) of 1,5-cyclooctadiene (COD) (Scheme 23) [62]. At 80°C in toluene, quantitative formation of poly (1,4-butadiene) was generated in less than 1 h from the ROMP of COD. Oxidation by 2,3-dichloro-5,6-dicyanoquinone (DDQ) resulted in a significant decrease in catalytic activity, and subsequent reduction by decamethylferrocene restored catalytic activity. As with the previously mentioned study [61], the weaker electron density at the metal center of the oxidized catalyst is believed to be the cause of its decreased catalytic activity.

One of the most important applications of switchable catalysis has been in polymerization. Nearly a decade after the first redox-active system for olefin polymerization was proposed, the viability of a ferrocene-containing Fe-Ti heterobimetallic complex to function as a switchable redox-active polymerization catalyst was demonstrated [63, 64]. Moreover, the authors investigated the effects of location of the redox-active moiety on catalysis.

Contrary to a previously reported Fe-Ti polymerization catalyst in which the ferrocenyl moiety is located distal to the Ti metal center [64], an Fe-Ti catalyst was synthesized in which the ferrocenyl moiety is proximal to the active Ti metal center

Scheme 24 Comparison of catalysts containing a redox-active ferrocenyl moiety proximal to the metal center (red; right) and ferrocenyl moieties distal to the metal center (purple; left)

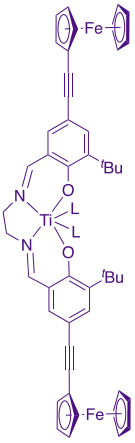

Gibson and Long., 2006

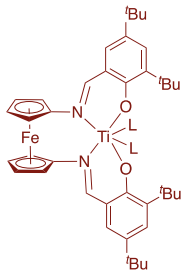

Long et al., 2015

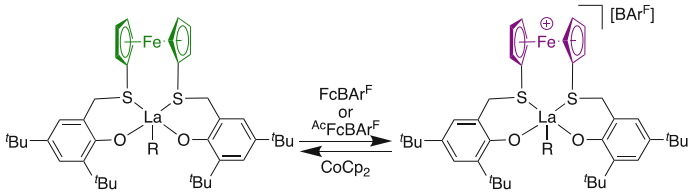

Scheme 25 Thiol-containing La-Fe catalysts

(Scheme 24). The authors found not only that their proximal ferrocenyl-containing heterobimetallic catalyzed the redox-switchable polymerization of LA, but also that the positioning of the redox-active ferrocenyl moiety in closer proximity to the active Ti metal center resulted in an improved redox switch in polymerization activity compared to the previously reported Fe-Ti catalyst.

The following year, two heterobimetallic thiol-containing La-Fe catalysts were synthesized in an effort to expand redox-switchable catalysts to include rare-earth-metal analogues as well as to investigate the effect of non-alkoxide versus alkoxide ancillary ligands on catalytic performance (Scheme 25) [65].

In their investigation, the authors found that both catalysts **A** and **B** were more active for ROP of *rac*-LA (*rac*-lactide) than their oxidized counterparts ($\mathbf{A_{ox}}$/$\mathbf{B_{ox}}$), with **A** achieving higher percent monomer conversion than **B**. As such, their results suggest that both non-alkoxide and alkoxide ancillary ligands may be employed for these redox-switchable catalysts while those catalysts containing non-alkoxide moieties might result in lower polymerization rates.

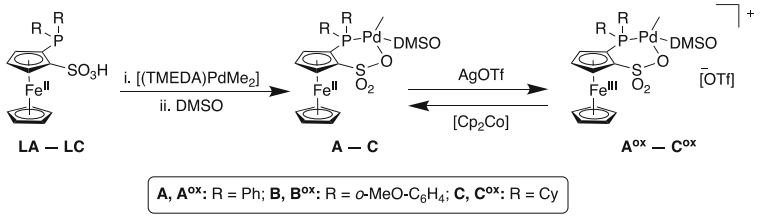

Scheme 26 Synthesis of 3 analogous redox-switchable Pd-Fe heterobimetallics

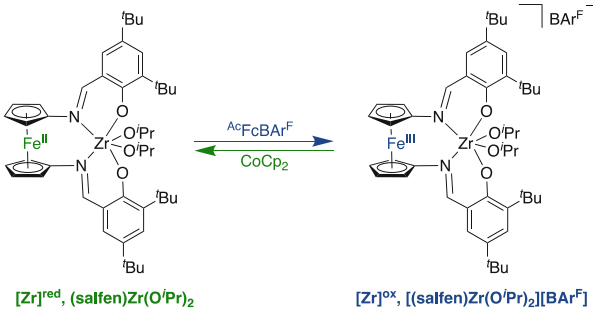

Scheme 27 Interconversion between [Fe-Zr]^{red} and [Fe-Zr]^{ox} redox states of redox-switchable Fe-Zr catalyst

Also in 2016, a set of 3 analogous redox-switchable Pd-Fe heterobimetallic complexes was reported that catalyze the copolymerization of olefins including norbornene oligomerization, ethylene homopolymerization, and ethylene/methyl acrylate copolymerization (Scheme 26) [66].

The catalytic activity of these heterobimetallics is controllable via redox switching. Particularly in norbornene oligomerization, the neutral heterobimetallic complexes were catalytically inactive while the oxidized complexes displayed significant catalytic activity. Hence, switching between the neutral and oxidized states in situ leads to corresponding on and off switching for norbornene oligomerization.

In 2019, the ability of an Fe-Zr heterobimetallic to function as a redox-switchable catalyst for the ring-opening polymerization and copolymerization of cyclic esters and ethers was detailed (Scheme 27) [67].

The authors tested several monomers for homopolymerization reactions with both the reduced [Fe-Zr]^{red} and oxidized [Fe-Zr]^{ox} states of the catalyst. CHO and PO (propylene oxide) were polymerizable via [Fe-Zr]^{ox}, while LA, VL, and TMC were polymerizable via [Fe-Zr]^{red}. Additionally, 16e block- and triblock-copolymers were synthesized by the redox-switchable Fe-Zr catalyst.

Later in 2019, an Fe-Al heterobimetallic complex was reported that functions as a redox-switchable catalyst for the ring-opening polymerization of cyclic esters and cyclohexene oxide (Scheme 28) [68].

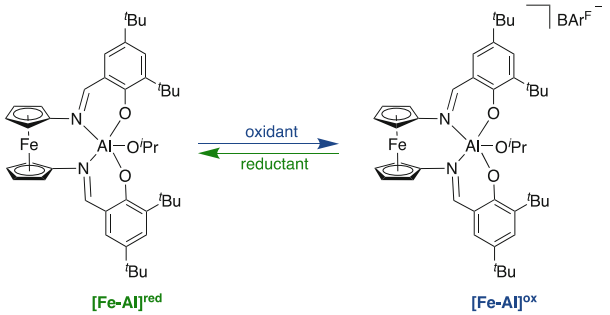

Scheme 28 Redox-switchable Fe-Al heterobimetallic polymerization catalyst. Note $[Fe\text{-}Al]^{red}$ is reduced state, and $[Fe\text{-}Al]^{ox}$ is oxidized state

Scheme 29 Synthesis of redox-switchable Au-Fe heterobimetallic cyclization catalyst

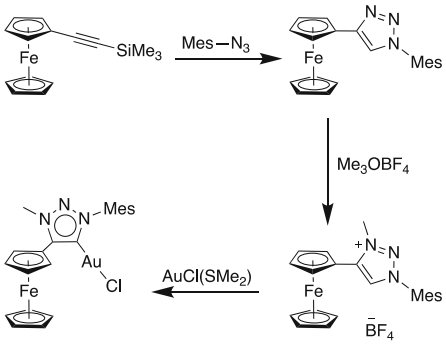

$[Fe\text{-}Al]^{red}$ polymerized LA (L-lactide), TMC (1,3-trimethylene carbonate), and BBL (b-butyrolactone), while $[Fe\text{-}Al]^{ox}$ did not. In fact, the only observed activity for $[Fe\text{-}Al]^{ox}$ was with CHO (cyclohexene oxide), and there was no observed selectivity between the two redox states for CL (e-caprolactone) and VL (d-valerolactone). Finally, the successful synthesis of AB and ABC-type block copolymers of CHO, TMC, and LA was performed via switching redox states of the Fe-Al heterobimetallic and sequential monomer addition.

Despite the prevalence of systems developed with polymerization applications in mind, redox-switchable metallocenes have been employed in a range of other reaction manifolds. A ferrocenyl-substituted mesoionic carbene-containing Au-Fe heterobimetallic complexes was presented in 2015 (Scheme 29) [69].

The authors were able to demonstrate that the oxidized form of the catalyst $[Au\text{-}Fe]^{ox}$ catalyzes the cyclization of *N*(2-propyn-1-yl)benzamide to 5-methylene-2-phenyl-4,5-dihydrooxazole while the unoxidized neutral form reduced [Au-Fe] was catalytically inactive (Scheme 30).

This shows that oxidation of the catalyst can be used to switch the catalyst on and off. Also of note, this report represents the first example of a heterobimetallic complex containing a redox-active ferrocenyl-triazolylidene metalloligand.

The ability of an Fe-Co heterobimetallic to catalyze the hydroalkoxylation of styrenes has been demonstrated as well (Scheme 31) [70].

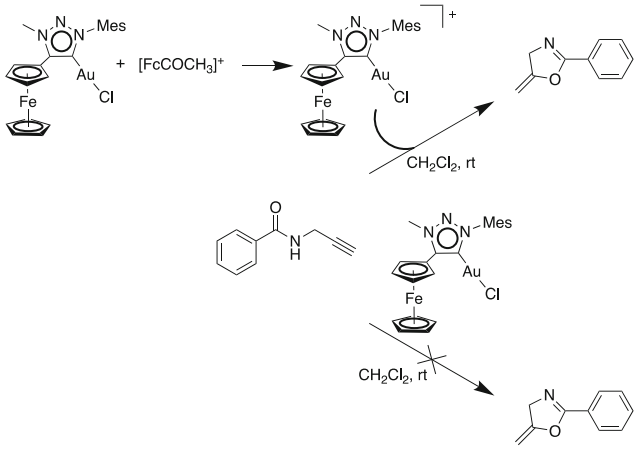

Scheme 30 Redox-switchable formation of 4,5-dihydrooxazole catalyzed by [Au-Fe]^{ox}

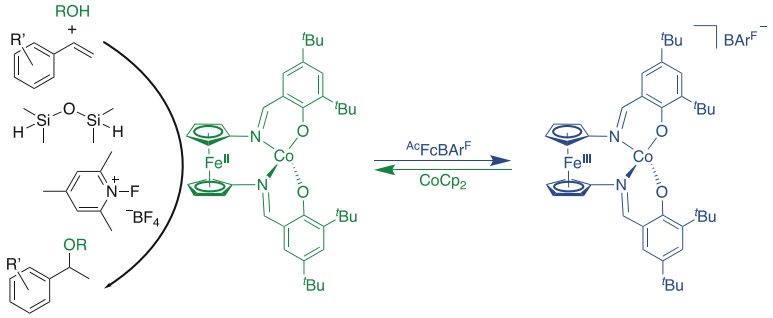

Scheme 31 Fe-Co heterobimetallic hydroalkoxylation catalyst

The one-electron-oxidized species was shown to be inactive toward hydroalkoxylation, and, as such, the hydroalkoxylation reactivity is able to be switched on and off in situ via redox chemistry.

Recently, the potential utility of this scaffold was demonstrated to extend beyond solely polymerization into additional reaction systems. In 2019, the ability of a sulfur-containing Fe-Zr heterobimetallic complex to function as a redox-switchable catalyst for intramolecular hydroamination was discovered (Scheme 32) [71].

The authors found that the reduced form of the complex catalyzes the hydroamination of primary aminoalkenes. Contrarily, the oxidized state of the heterobimetallic was shown to catalyze the hydroamination of secondary aminoalkenes. By switching between the two redox states, they were able to selectively catalyze primary aminoalkene hydroamination over secondary, and vice versa.

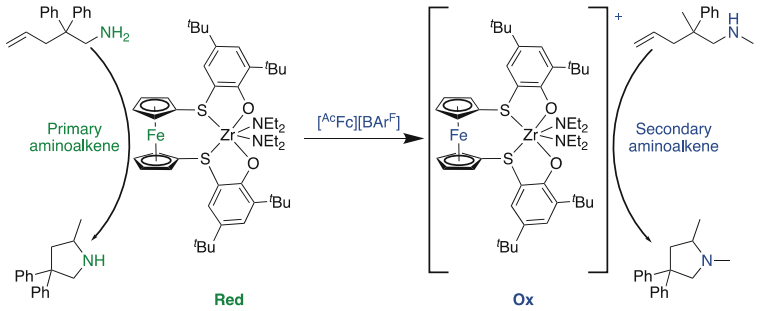

Scheme 32 Redox-switchable Fe-Zr heterobimetallic catalyst for hydroamination reactions

Scheme 33 Structure of Th_2-arene (arene: benzene, naphthalene, anthracene)

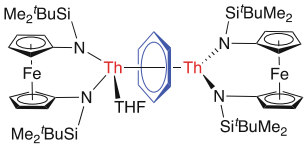

Most recently, in late 2020, dimeric Th-Fe heterobimetallics (Th_2-arene; arene: benzene, naphthalene, anthracene) were shown to reduce select arenes as well as alkynes (Scheme 33) [72].

It was found that all Th_2-arene served as reductants for azobenzene or cyclooctatetraene. Interestingly, all Th_2-arene were able to reduce diphenylacetylene, yet only the most reactive Th_2-naph could reduce bis (trimethylsilyl)acetylene (Scheme 34).

In 2016, an Fe-Au heterobimetallic complex was revealed to have the ability to behave as a redox-switchable catalyst for alkyne cyclization with furans (Scheme 35) [73].

It was determined that the neutral heterobimetallic $[Fe\text{-}Au]^{neut}$ was catalytically inactive. However, upon addition of acetylferrocenium tetrafluoroborate as the oxidant, the oxidized form of the heterobimetallic complex $[Fe\text{-}Au]^{ox}$ generated moderate to good yields of the final products (Scheme 36).

The authors attribute the catalytic activity of the oxidized heterobimetallic catalyst $[Fe\text{-}Au]^{ox}$ to the increased electrophilicity of the Au metal center resulting from the production of a cationic ligand due to oxidation. Thus, switching from neutral $[Fe\text{-}Au]^{neut}$ to oxidized $[Fe\text{-}Au]^{ox}$ affords a corresponding switch in alkyne cyclization catalysis from off to on.

A subsequent report detailed an Ru-Fe heterobimetallic complex analogous to their previously reported Fe-Au system (Scheme 37) [74]. The investigators discovered that the Ru-Fe heterobimetallic complex [Ru-Fe] functions as a redox-switchable catalyst for the transfer hydrogenation of imines and ketones. It was found that, while the neutral heterobimetallic [Ru-Fe] was highly active for reducing

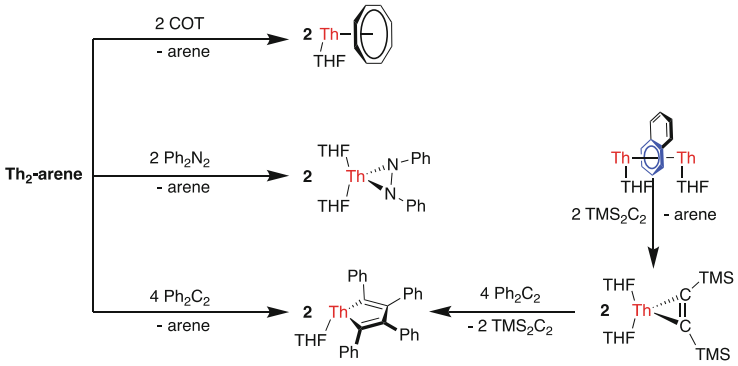

Scheme 34 Reduction reactivity studies of Th_2-arene

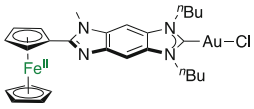

Scheme 35 Redox-switchable Fe-Au heterobimetallic catalyst in neutral state $[Fe\text{-}Au]^{neut}$

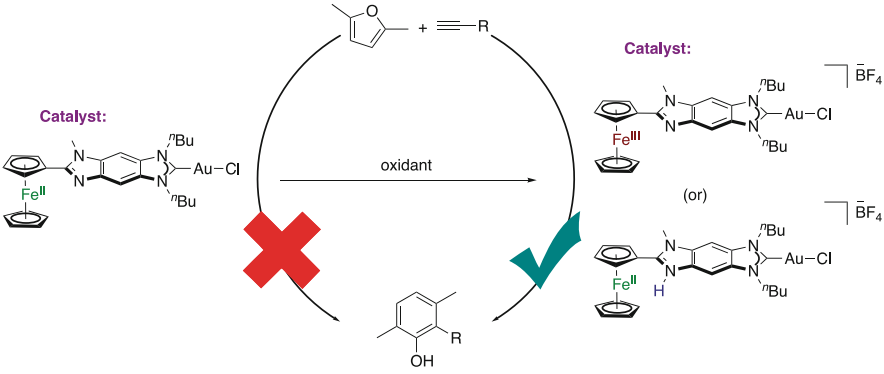

Scheme 36 Effect of redox switching on catalysis of alkyne cyclization with furans

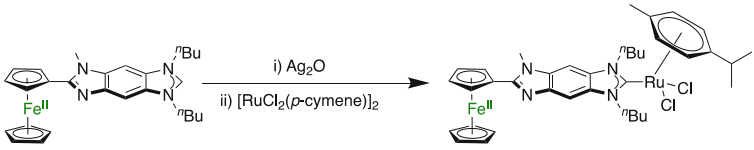

Scheme 37 Synthesis of Ru-Fe heterobimetallic catalyst [Ru-Fe] for transfer hydrogenation

Table 1 Transfer hydrogenation of imines and ketones using redox-switchable [Ru-Fe][a]

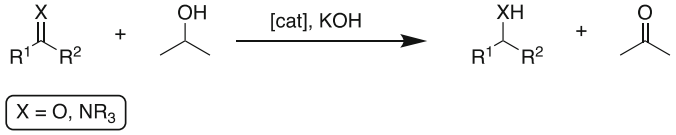

Entry	Substrate	Catalyst	Yield [%][b]
1	acetophenone	**[Ru-Fe]**	94
2	acetophenone	**[Ru-Fe]** + oxidant	24
3	cyclohexanone	**[Ru-Fe]**	75
4	cyclohexanone	**[Ru-Fe]** + oxidant	66
5	hexanophenone	**[Ru-Fe]**	94
6	hexanophenone	**[Ru-Fe]** + oxidant	20
7	2-acetophenone	**[Ru-Fe]**	60
8	2-acetophenone	**[Ru-Fe]** + oxidant	6
9	4-bromoacetophenone	**[Ru-Fe]**	68
10	4-bromoacetophenone	**[Ru-Fe]** + oxidant	51
11	4-methoxyacetophenone	**[Ru-Fe]**	40
12	4-methoxyacetophenone	**[Ru-Fe]** + oxidant	18
13	*N*-benzylideneaniline	**[Ru-Fe]**	85
14	*N*-benzylideneaniline	**[Ru-Fe]** + oxidant	81

[a] Reaction conditions: 0.5 mmol ketone or imine, 0.05 mmol KOH, 0.5 mol% of [Ru-Fe], 0.5 mol% of acetylferrocenium tetrafluoroborate (oxidant), and 2 mL of isopropanol at 80°C for 2 h
[b] Yields determined by GC using anisole (0.5 mmol) as an internal standard

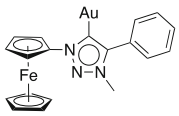

Scheme 38 Redox-switchable Au-Fe heterobimetallic cyclization catalyst

all tested substrates, the oxidized species [Ru-Fe]^{ox} showed reduced activity for ketone reduction (Table 1).

Moreover, the authors demonstrated that the rate of hexaphenone reduction could actually be modulated via addition of subsequent amounts of reductant and oxidant. Addition of acetylferrocenium tetrafluoroborate (oxidant) leads to decreased catalytic activity, while subsequent addition of cobaltocene (reductant) leads to restoration of catalytic activity to pre-oxidation levels.

The first example of redox-switchable catalysis with a gold(I) complex was described in a 2017 report on an Au-Fe heterobimetallic (Scheme 38) [75].

The authors demonstrated the ability of their Au-Fe heterobimetallic to catalyze cyclization reactions, including the formation of furan, phenol, and oxazoline (Scheme 39).

Scheme 39 Formation of oxazoline (top), furan (middle), and phenol (bottom) catalyzed by redox-switchable [Au-Fe]

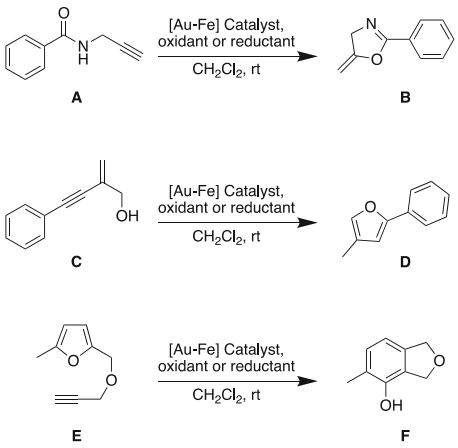

Scheme 40 Back and forth switching during [Au-Fe] catalyzed phenol formation

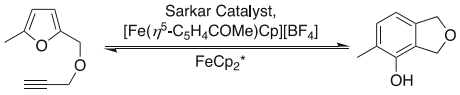

Scheme 41 Redox-switchable Rh-Fe catalyst for terminal alkyne hydrosilylation

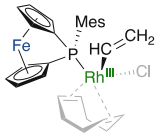

Moreover, the authors showed that switching from the unoxidized native form of the catalyst [Au-Fe] to the oxidized form $[Au\text{-}Fe]^{ox}$ turns the catalytic activity from off to on, respectively. In addition, the addition of decamethylferrocene to the active catalyst $[Au\text{-}Fe]^{ox}$ is shown to turn catalysis back off via reduction back to the native unoxidized heterobimetallic [Au-Fe]. Interestingly, in the case of the phenol formation, a different kind of switching was observed. As with the furan and oxazoline formation before, $[Au\text{-}Fe]^{ox}$ leads to phenol formation. However, reduction with decamethylferrocene leads to back-conversion of the phenol to starting material (Scheme 40).

Independent control experiments suggest this back and forth switching is inherently connected to the entire catalytic mixture.

The same year, an Rh-Fe heterobimetallic that serves as a redox-responsive catalyst for hydrosilylation of terminal alkynes was also reported (Scheme 41) [76]. It was shown that all hydrosilylation reactions were drastically accelerated with the catalyst in its oxidized form $[Rh\text{-}Fe]^{ox}$ instead of its reduced form $[Rh\text{-}Fe]^{red}$. Perhaps even more significantly, the authors discovered that both the selectivity and the product distribution of the catalysis changed appreciably upon switching from $[Rh\text{-}Fe]^{ox}$ to $[Rh\text{-}Fe]^{red}$.

Scheme 42 Redox-responsive Au-Fe heterobimetallic catalyst for alkyne hydroamination

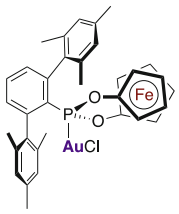

More recently, in 2019, a redox-responsive Au-Fe heterobimetallic complex was described that catalyzed alkyne hydroamination (Scheme 42) [77]. The authors discovered that the hydroamination reaction generally occurs approximately two times faster when the catalyst is switched to its oxidized form $[Au\text{-}Fe]^{ox}$ instead of its reduced form $[Au\text{-}Fe]^{red}$.

Additionally, the researchers examined the hydroamination of electron-poor, electron-rich, and aliphatic alkynes in their study and found that the electronic nature of the alkyne actually had a meaningful impact on the efficiency of the reaction, with electron-donating groups slowing the reaction down (Table 2).

Similar to the aforementioned work, a redox-switchable Au-Fe heterobimetallic cyclization catalyst was recently reported (Scheme 43) [78].

The authors demonstrated that, while the oxidized heterobimetallic $[Au\text{-}Fe]^{ox}$ was catalytically active for the cyclization of N(2-propyn-1-yl)benzamide to 2-phenyl-5-vinylidene-2-oxazoline, the reduced form $[Au\text{-}Fe]^{red}$ is inactive. Further, redox switching between $[Au\text{-}Fe]^{ox}$ and $[Au\text{-}Fe]^{red}$ switches catalytic turnover on and off.

3.1.2 Cation-Responsive Systems

In 2014, a heterobimetallic Ir-crown ether complex, in which the crown either moiety contains either Na^+ or Li^+, was reported to catalyze H_2 activation and facilitate H/D exchange (Scheme 44) [79].

The main-group cation is thought to sequester the crown ether and prevent an oxygen atom from competing with H_2 for an open site at the iridium center. Interestingly, it was determined that the rate of H_2 activation can be controlled by cation selection. Reactions containing lithium proceed approximately 10 times faster than those reactions involving sodium. Moreover, the H/D exchange reaction rate can be increased up to 250-fold upon addition of catalytic amounts of Li^+. Thus, modification of the identity and concentration of the main-group cation results in corresponding modification of the reaction.

This type of cation-responsive system has been extended beyond hydrogen activation and into the field of olefin isomerization [80]. Simple halide abstraction switched the monometallic Ir catalyst from inactive to active (i.e., off to on) (Scheme 45).

From that point, it was found that the catalyst activity could be tuned by converting the monometallic Ir catalyst to a heterobimetallic Ir-M (M = K, Na, Li)

Table 2 Scope of alkyne hydroamination catalyzed by Au-Fe

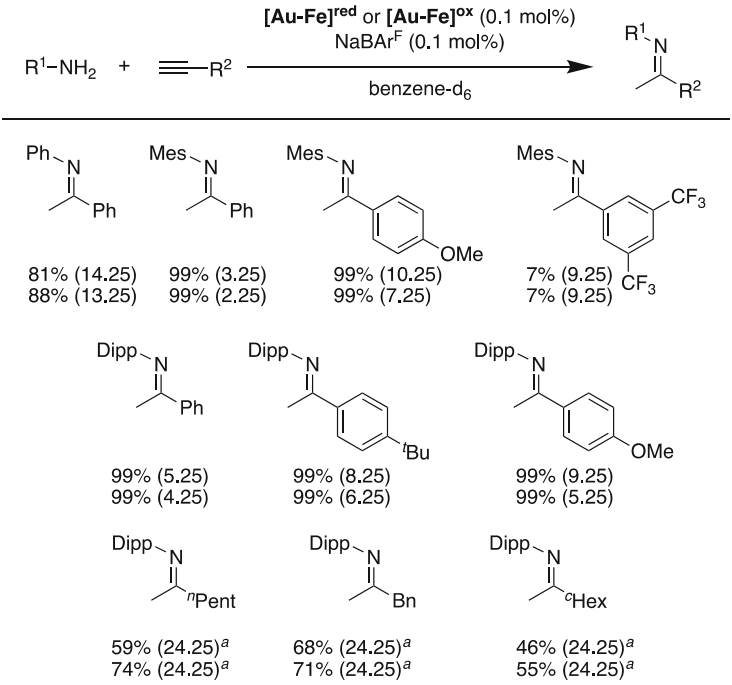

Hydroamination of alkynes. Yields are given for [Au-Fe]^{red} (upper value) and [Au-Fe]^{ox} (lower value); numbers in parentheses correspond to reaction times in [h]. Reactions were conducted on a 0.1 mmol scale in d_6-benzene with 0.1 mol% [Au-Fe]^{red} and 0.1 mol% $NaBAr^F$ as activating agents. [Au-Fe]^{ox} was generated in situ prior to the reaction by addition of 0.1 mol% [Fc(Oac)][Al{OC$(CF_3)_3$}$_4$]. The yields were determined using 1,3,5-$(MeO)_3C_6H_3$ as an internal standard

[a] Reactions were conducted using a 1 mol% catalyst/activator

Scheme 43 Switchable gold-catalyzed cyclization of *N*(2-propyn-1-yl) benzamide to 2-phenyl-5-vinylidene-2-oxazoline

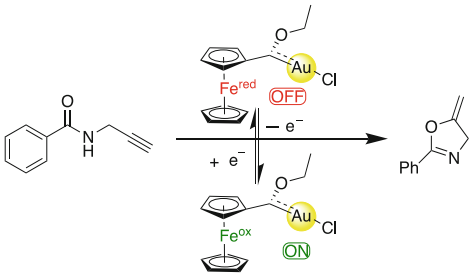

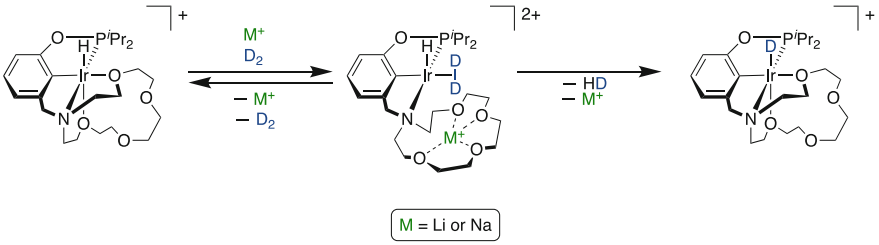

Scheme 44 Overall H_2 activation and H/D exchange reaction

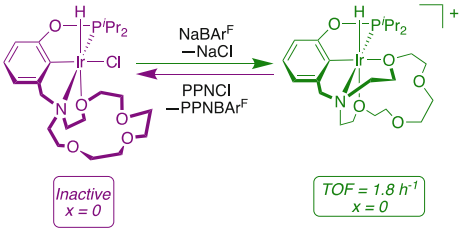

Scheme 45 Interconversion between inactive (purple; left) and active (green; right) olefin isomerization catalyst

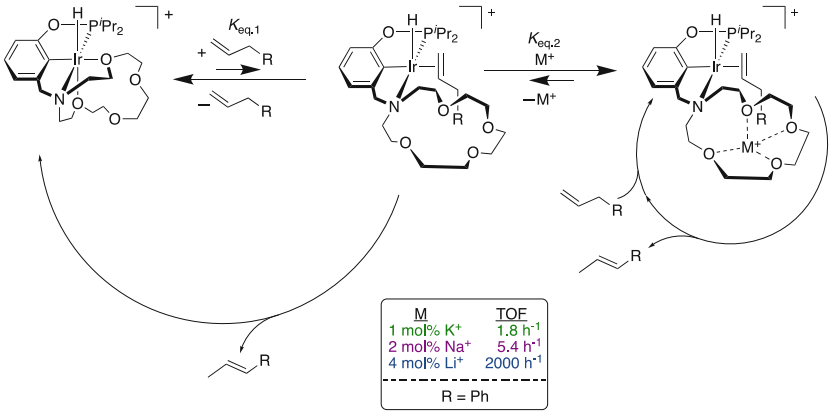

Scheme 46 Proposed mechanism for cation-controlled olefin isomerization via heterobimetallic catalysis

catalyst via addition of main-group metal salts. Turnover frequency (TOF) for olefin isomerization increased upon changing M such that TOF: K < Na < Li (Scheme 46).

Further still, the authors demonstrated that addition of chloride salts completely halts catalytic activity, allowing for the catalyst to be switched off and on using chloride salts (off) and sodium salts (on).

It is also worth noting that redox-switchable catalytic ability of crown ether-containing Ir-M (M = metal salt) heterobimetallic complexes extends to modulate methanol carbonylation [81, 82]. In these systems, structurally analogous to previously mentioned heterobimetallics [79, 80], changing the metal cation results in corresponding changes to the turnover number (TON) for the methanol carbonylation. Rather than a simple on and off switch, the authors demonstrate the potential for cation-controlled reaction tunability.

4 Conclusions

As displayed throughout this chapter, a specific class of heterobimetallic complexes in which each metal center resides in the second coordination sphere of the other has recently emerged as an area of increased interest. This is undoubtedly due to the unique reactivity manifolds afforded by these complexes as a result of the presence of two different metal centers. Stoichiometric bond activation is observed in heterobimetallic species that is otherwise not seen without both metals present. In some examples, activation is achieved in a manner not dissimilar to Lewis pair-type chemistry in which the two metals form an adduct with a new M–M' bond following bond activation. Catalytic bond activation ranging from alkenylation to polymerization facilitated by these heterobimetallics has been observed, with some examples showing regioselectivity. Ongoing progress continues in the development of catalytically useful second-sphere bimetallic systems. Of particular note is the recent emergence of switchable heterobimetallic complexes. In this chapter, we have discussed both redox-switchable and cation-responsive heterobimetallic systems.

In redox-switchable systems, changing the oxidation state of one of the metals is used to modify catalytic activity. In many systems, oxidizing or reducing one of the metals switches catalysis from "off" to "on" and vice versa. While polymerization is the centerpiece of redox-switchable heterobimetallics, switchable systems have had application in additional reactions such as alkyne cyclization, hydroamination, and hydrosilylation. Similarly, cation-responsive systems utilize cation manipulation to influence catalytic activity with some evidence to suggest size of the cation could have an appreciable effect on catalysis. Future directions in this area include the generation of "multi-state" switches, systems that can exist in states beyond the currently standard "on" and "off."

Though perhaps not as commonly encountered for bond activation and catalysis as systems containing formal metal–metal bonds, the field of second-sphere bimetallic chemistry is certain to grow over the coming years. Potential applications are limitless, as the metals can function cooperatively or in tandem to achieve desired reactivity. We look forward to watching the field mature and are excited for what is yet to come!

References

1. Stephan DW (1989) Early-late heterobimetallics. Coord Chem Rev 95(1):41–107. https://doi.org/10.1016/0010-8545(89)80002-5
2. Charles III RM, Brewster TP (2021) H2 and carbon-heteroatom bond activation mediated by polarized heterobimetallic complexes. Coord Chem Rev 433:213765. https://doi.org/10.1016/j.ccr.2020.213765
3. Cotton FA, Lecture C (1975) Quadruple bonds and other multiple metal to metal bonds. Chem Soc Rev 4(1):27–53. https://doi.org/10.1039/CS9750400027
4. Cotton FA (1978) Discovering and understanding multiple metal-to-metal bonds. Acc Chem Res 11(6):225–232. https://doi.org/10.1021/ar50126a001
5. Cooper BG, Napoline JW, Thomas CM (2012) Catalytic applications of early/late heterobimetallic complexes. Catal Rev 54(1):1–40. https://doi.org/10.1080/01614940.2012.619931
6. Wheatley N, Kalck P (1999) Structure and reactivity of early−late heterobimetallic complexes. Chem Rev 99(12):3379–3420. https://doi.org/10.1021/cr980325m
7. Campos J (2020) Bimetallic cooperation across the periodic table. Nat Rev Chem 4(12):696–702. https://doi.org/10.1038/s41570-020-00226-5
8. Park J, Hong S (2012) Cooperative bimetallic catalysis in asymmetric transformations. Chem Soc Rev 41(21):6931–6943. https://doi.org/10.1039/C2CS35129C
9. Hicks J, Vasko P, Goicoechea JM, Aldridge S (2018) Synthesis, structure and reaction chemistry of a nucleophilic aluminyl anion. Nature 557(7703):92–95. https://doi.org/10.1038/s41586-018-0037-y
10. Charles III RM, Yokley TW, Schley ND, DeYonker NJ, Brewster TP (2019) Hydrogen activation and hydrogenolysis facilitated by late-transition-metal–aluminum heterobimetallic complexes. Inorg Chem 58(19):12635–12645. https://doi.org/10.1021/acs.inorgchem.9b01359
11. Brewster TP, Nguyen TH, Li Z, Eckenhoff WT, Schley ND, DeYonker NJ (2018) Synthesis and characterization of heterobimetallic iridium–aluminum and rhodium–aluminum complexes. Inorg Chem 57(3):1148–1157. https://doi.org/10.1021/acs.inorgchem.7b02601
12. Stephan DW (2015) Frustrated Lewis pairs: from concept to catalysis. Acc Chem Res 48(2):306–316. https://doi.org/10.1021/ar500375j
13. Stephan DW (2016) The broadening reach of frustrated Lewis pair chemistry. Science 354(6317). https://doi.org/10.1126/science.aaf7229
14. Stephan DW, Erker G (2015) Frustrated Lewis pair chemistry: development and perspectives. Angew Chem Int Ed 54(22):6400–6441. https://doi.org/10.1002/anie.201409800
15. Bouhadir G, Bourissou D (2016) Complexes of ambiphilic ligands: reactivity and catalytic applications. Chem Soc Rev 45(4):1065–1079. https://doi.org/10.1039/C5CS00697J
16. Flynn SR, Wass DF (2013) Transition metal frustrated Lewis pairs. ACS Catal 3(11):2574–2581. https://doi.org/10.1021/cs400754w
17. Navarro M, Campos J (2021) Chapter three – bimetallic frustrated Lewis pairs. In: Pérez PJ (ed) Advances in organometallic chemistry, vol 75. Academic Press, pp 95–148. https://doi.org/10.1016/bs.adomc.2021.01.001
18. Devillard M, Declercq R, Nicolas E, Ehlers AW, Backs J, Saffon-Merceron N, Bouhadir G, Slootweg JC, Uhl W, Bourissou D (2016) A significant but constrained geometry Pt→Al interaction: fixation of CO2 and CS2, activation of H2 and PhCONH2. J Am Chem Soc 138(14):4917–4926. https://doi.org/10.1021/jacs.6b01320
19. Shima T, Suzuki H (2005) Heterobimetallic polyhydride complex, Cp*Ru(μ-H)4OsCp* (Cp* = H5-C5Me5). Synthesis and reaction with ethylene. Organometallics 24(16):3939–3945. https://doi.org/10.1021/om0503996
20. Suzuki H, Omori H, Moro-Oka Y (1988) Activation of the carbon-hydrogen bond of ethylene by a dinuclear tetrahydride-bridged ruthenium complex. Organometallics 7(12):2579–2581. https://doi.org/10.1021/om00102a031

21. Omori H, Suzuki H, Morooka Y (1989) Preparation and structure determination of a dinuclear ruthenacyclopentadiene complex. Coupling of coordinated vinyl ligands. Organometallics 8(6): 1576–1578. https://doi.org/10.1021/om00108a039
22. Suzuki H, Omori H, Lee DH, Yoshida Y, Fukushima M, Tanaka M, Moro-oka Y (1994) Synthesis, structure, and chemistry of a dinuclear tetrahydride-bridged complex of ruthenium, (. Eta.5-C5Me5)Ru(.Mu.-H)4Ru(.Eta.5-C5Me5). C-H bond activation and coupling reaction of ethylene on dinuclear complexes. Organometallics 13(4):1129–1146. https://doi.org/10.1021/om00016a017
23. Oishi M, Kato T, Nakagawa M, Suzuki H (2008) Synthesis and reactivity of early−late heterobimetallic hydrides of group 4 metals and iridium supported by mono(H5-C5Me5) ancillary ligands: bimetallic carbon−hydrogen bond activation. Organometallics 27(23): 6046–6049. https://doi.org/10.1021/om800715b
24. Cai Z, Xiao D, Do LH (2019) Cooperative heterobimetallic catalysts in coordination insertion polymerization. Comments Inorg Chem 39(1):27–50. https://doi.org/10.1080/02603594.2019.1570165
25. Boulho C, Zijlstra HS, Harder S (2015) Oxide-bridged heterobimetallic aluminum/zirconium catalysts for ethylene polymerization. Eur J Inorg Chem 2015(12):2132–2138. https://doi.org/10.1002/ejic.201500123
26. Boulho C, Zijlstra HS, Hofmann A, Budzelaar PHM, Harder S (2016) Insight into oxide-bridged heterobimetallic Al/Zr olefin polymerization catalysts. Chem Eur J 22(48): 17450–17459. https://doi.org/10.1002/chem.201602674
27. Chiu H-C, Koley A, Dunn PL, Hue RJ, Tonks IA (2017) Ethylene polymerization catalyzed by bridging Ni/Zn heterobimetallics. Dalton Trans 46(17):5513–5517. https://doi.org/10.1039/C7DT00222J
28. Nakamura T, Suzuki K, Yamashita M (2018) A Zwitterionic aluminabenzene–alkylzirconium complex having half-zirconocene structure: synthesis and application for additive-free ethylene polymerization. Chem Commun 54(33):4180–4183. https://doi.org/10.1039/C8CC02186D
29. Bhattacharjee H, Müller J (2016) Metallocenophanes bridged by group 13 elements. Coord Chem Rev 314:114–133. https://doi.org/10.1016/j.ccr.2015.09.008
30. Suo H, Solan GA, Ma Y, Sun W-H (2018) Developments in compartmentalized bimetallic transition metal ethylene polymerization catalysts. Coord Chem Rev 372:101–116. https://doi.org/10.1016/j.ccr.2018.06.006
31. Tanabiki M, Tsuchiya K, Motoyama Y, Nagashima H (2005) Monometallic and heterobimetallic azanickellacycles as ethylene polymerization catalysts. Chem Commun 27: 3409–3411. https://doi.org/10.1039/B502942B
32. Gurubasavaraj PM, Nomura K (2010) Hetero-bimetallic complexes of titanatranes with aluminum alkyls: synthesis, structural analysis, and their use in catalysis for ethylene polymerization. Organometallics 29(16):3500–3506. https://doi.org/10.1021/om100119g
33. Kulangara SV, Jabri A, Yang Y, Korobkov I, Gambarotta S, Duchateau R (2012) Synthesis, X-ray structural analysis, and ethylene polymerization studies of group IV metal heterobimetallic aluminum-pyrrolyl complexes. Organometallics 31(17):6085–6094. https://doi.org/10.1021/om300453a
34. Barisic D, Lebon J, Maichle-Mössmer C, Anwander R (2019) Pentadienyl migration and abstraction in yttrium aluminabenzene complexes including a single-component catalyst for isoprene polymerization. Chem Commun 55(49):7089–7092. https://doi.org/10.1039/C9CC02857A
35. Barisic D, Buschmann DA, Schneider D, Maichle-Mössmer C, Anwander R (2019) Rare-earth-metal pentadienyl half-sandwich and sandwich tetramethylaluminates–synthesis, structure, reactivity, and performance in isoprene polymerization. Chem A Eur J 25(18):4821–4832. https://doi.org/10.1002/chem.201900108
36. Tritto I, Li SX, Sacchi MC, Locatelli P, Zannoni G (1995) Titanocene-Methylaluminoxane catalysts for olefin polymerization: a 13C NMR study of the reaction equilibria and polymerization. Macromolecules 28(15):5358–5362. https://doi.org/10.1021/ma00119a028

37. Fischer D, Mülhaupt R (1994) The influence of Regio- and Stereoirregularities on the crystallization behaviour of isotactic poly(propylene)s prepared with homogeneous group IVa metallocene/Methylaluminoxane Ziegler-Natta catalysts. Macromol Chem Phys 195(4): 1433–1441. https://doi.org/10.1002/macp.1994.021950426
38. Endo K, Uchida Y, Matsuda Y (1996) Polymerizations of butadiene with Ni(Acac)2-methylaluminoxane catalysts. Macromol Chem Phys 197(11):3515–3521. https://doi.org/10.1002/macp.1996.021971102
39. Endo K, Yamanaka Y (2001) Polymerization of butadiene with V(Acac)3-methylaluminoxane catalyst. Macromol Chem Phys 202(1):201–206. https://doi.org/10.1002/1521-3935(20010101)202:1<201::AID-MACP201>3.0.CO;2-D
40. Wang J, Li H, Guo N, Li L, Stern CL, Marks TJ (2004) Covalently linked heterobimetallic catalysts for olefin polymerization. Organometallics 23(22):5112–5114. https://doi.org/10.1021/om049481b
41. Ishino H, Takemoto S, Hirata K, Kanaizuka Y, Hidai M, Nabika M, Seki Y, Miyatake T, Suzuki N (2004) Olefin polymerization catalyzed by titanium−tungsten heterobimetallic dinitrogen Complexes1. Organometallics 23(20):4544–4546. https://doi.org/10.1021/om049447x
42. Liu S, Motta A, Mouat AR, Delferro M, Marks TJ (2014) Very large cooperative effects in heterobimetallic titanium-chromium catalysts for ethylene polymerization/copolymerization. J Am Chem Soc 136(29):10460–10469. https://doi.org/10.1021/ja5046742
43. Tsai C-C, Shih W-C, Fang C-H, Li C-Y, Ong T-G, Yap GPA (2010) Bimetallic nickel aluminun mediated para-selective alkenylation of pyridine: direct observation of H2,H1-pyridine Ni(0)−Al(III) intermediates prior to C−H bond activation. J Am Chem Soc 132(34):11887–11889. https://doi.org/10.1021/ja1061246
44. Nakao Y, Yamada Y, Kashihara N, Hiyama T (2010) Selective C-4 alkylation of pyridine by nickel/Lewis acid catalysis. J Am Chem Soc 132(39):13666–13668. https://doi.org/10.1021/ja106514b
45. Nakao Y, Morita E, Idei H, Hiyama T (2011) Dehydrogenative [4 + 2] cycloaddition of formamides with alkynes through double C−H activation. J Am Chem Soc 133(10): 3264–3267. https://doi.org/10.1021/ja1102037
46. Shih W-C, Chen W-C, Lai Y-C, Yu M-S, Ho J-J, Yap GPA, Ong T-G (2012) The regioselective switch for amino-NHC mediated C–H activation of benzimidazole via Ni–Al synergistic catalysis. Org Lett 14(8):2046–2049. https://doi.org/10.1021/ol300570f
47. Yang L, Uemura N, Nakao Y (2019) Meta-selective C–H borylation of benzamides and pyridines by an Iridium–Lewis acid bifunctional catalyst. J Am Chem Soc 141(19): 7972–7979. https://doi.org/10.1021/jacs.9b03138
48. Osipova ES, Gulyaeva ES, Gutsul EI, Kirkina VA, Pavlov AA, Nelyubina YV, Rossin A, Peruzzini M, Epstein LM, Belkova NV, Filippov OA, Shubina ES (2021) Bifunctional activation of amine-boranes by the W/Pd bimetallic analogs of "Frustrated Lewis Pairs". Chem Sci 12(10):3682–3692. https://doi.org/10.1039/D0SC06114J
49. Buil ML, Esteruelas MA, Izquierdo S, Nicasio AI, Oñate E (2020) N–H and C–H bond activations of an isoindoline promoted by iridium- and osmium-polyhydride complexes: a noninnocent bridge ligand for acceptorless and base-free dehydrogenation of secondary alcohols. Organometallics 39(14):2719–2731. https://doi.org/10.1021/acs.organomet.0c00316
50. Yin G, Li Y, Wang R-H, Li J-F, Xu X-T, Luan Y-X, Ye M (2021) Ligand-controlled Ni(0)–Al(III) bimetal-catalyzed C3–H alkenylation of 2-pyridones by reversing conventional selectivity. ACS Catal 11(8):4606–4612. https://doi.org/10.1021/acscatal.1c00750
51. Donets PA, Cramer N (2013) Diaminophosphine oxide ligand enabled asymmetric nickel-catalyzed hydrocarbamoylations of alkenes. J Am Chem Soc 135(32):11772–11775. https://doi.org/10.1021/ja406730t
52. Slone CS, Mirkin CA, Yap GPA, Guzei IA, Rheingold AL (1997) Oxidation-state-dependent reactivity and catalytic properties of a Rh(I) complex formed from a redox-switchable hemilabile ligand. J Am Chem Soc 119(44):10743–10753. https://doi.org/10.1021/ja9723601

53. Lorkovic IM, Duff RR, Wrighton MS (1995) Use of the redox-active ligand 1,1'-bis (Diphenylphosphino)cobaltocene to reversibly alter the rate of the rhodium(I)-catalyzed reduction and isomerization of ketones and alkenes. J Am Chem Soc 117(12):3617–3618. https://doi.org/10.1021/ja00117a033
54. Schrock RR, Osborn JA (1970) Rhodium catalysts for the homogeneous hydrogenation of ketones. J Chem Soc D 9:567–568. https://doi.org/10.1039/C29700000567
55. Schrock RR, Osborn JA (1976) Catalytic hydrogenation using cationic rhodium complexes. I. Evolution of the catalytic system and the hydrogenation of olefins. J Am Chem Soc 98(8):2134–2143. https://doi.org/10.1021/ja00424a020
56. Tolman CA (1977) Steric effects of phosphorus ligands in organometallic chemistry and homogeneous catalysis. Chem Rev 77(3):313–348. https://doi.org/10.1021/cr60307a002
57. Jacobsen EN, Zhang W, Guler ML (1991) Electronic tuning of asymmetric catalysts. J Am Chem Soc 113(17):6703–6704. https://doi.org/10.1021/ja00017a069
58. RajanBabu TV, Casalnuovo AL (1992) Tailored ligands for asymmetric catalysis: the hydrocyanation of vinyl arenes. J Am Chem Soc 114(15):6265–6266. https://doi.org/10.1021/ja00041a066
59. RajanBabu TV, Ayers TA, Casalnuovo AL (1994) Electronic amplification of selectivity in rh-catalyzed hydrogenations: D-glucose-derived ligands for the synthesis of D- or L-amino acids. J Am Chem Soc 116(9):4101–4102. https://doi.org/10.1021/ja00088a065
60. Süßner M, Plenio H (2005) Redox-switchable phase tags for recycling of homogeneous catalysts. Angew Chem Int Ed 44(42):6885–6888. https://doi.org/10.1002/anie.200502182
61. Arumugam K, Varnado Jr CD, Sproules S, Lynch VM, Bielawski CW (2013) Redox-switchable ring-closing metathesis: catalyst design, synthesis, and study. Chem A Eur J 19(33):10866–10875. https://doi.org/10.1002/chem.201301247
62. Varnado Jr CD, Rosen EL, Collins MS, Lynch VM, Bielawski CW (2013) Synthesis and study of olefin metathesis catalysts supported by redox-switchable diaminocarbene[3] ferrocenophanes. Dalton Trans 42(36):13251–13264. https://doi.org/10.1039/C3DT51278A
63. Brown LA, Rhinehart JL, Long BK (2015) Effects of ferrocenyl proximity and monomer presence during oxidation for the redox-switchable polymerization of l-lactide. ACS Catal 5(10):6057–6060. https://doi.org/10.1021/acscatal.5b01434
64. Gregson CKA, Gibson VC, Long NJ, Marshall EL, Oxford PJ, White AJP (2006) Redox control within single-site polymerization catalysts. J Am Chem Soc 128(23):7410–7411. https://doi.org/10.1021/ja061398n
65. Hermans C, Rong W, Spaniol TP, Okuda J (2016) Lanthanum complexes containing a bis (phenolate) ligand with a ferrocene-1,1′-diyldithio backbone: synthesis, characterization, and ring-opening polymerization of Rac-lactide. Dalton Trans 45(19):8127–8133. https://doi.org/10.1039/C6DT00272B
66. Chen M, Yang B, Chen C (2015) Redox-controlled olefin (Co)polymerization catalyzed by ferrocene-bridged phosphine-sulfonate palladium complexes. Angew Chem Int Ed 54(51): 15520–15524. https://doi.org/10.1002/anie.201507274
67. Dai R, Diaconescu PL (2019) Investigation of a zirconium compound for redox switchable ring opening polymerization. Dalton Trans 48(9):2996–3002. https://doi.org/10.1039/C9DT00212J
68. Lai A, Hern ZC, Diaconescu PL (2019) Switchable ring-opening polymerization by a ferrocene supported aluminum complex. ChemCatChem 11(16):4210–4218. https://doi.org/10.1002/cctc.201900747
69. Hettmanczyk L, Manck S, Hoyer C, Hohloch S, Sarkar B (2015) Heterobimetallic complexes with redox-active mesoionic carbenes as metalloligands: electrochemical properties, electronic structures and catalysis. Chem Commun 51(54):10949–10952. https://doi.org/10.1039/C5CC01578B
70. Shepard SM, Diaconescu PL (2016) Redox-switchable hydroelementation of a cobalt complex supported by a ferrocene-based ligand. Organometallics 35(15):2446–2453. https://doi.org/10.1021/acs.organomet.6b00317

71. Shen Y, Shepard SM, Reed CJ, Diaconescu PL (2019) Zirconium complexes supported by a ferrocene-based ligand as redox switches for hydroamination reactions. Chem Commun 55(39): 5587–5590. https://doi.org/10.1039/C9CC01076A
72. Yu C, Liang J, Deng C, Lefèvre G, Cantat T, Diaconescu PL, Huang W (2020) Arene-bridged dithorium complexes: inverse sandwiches supported by a δ bonding interaction. J Am Chem Soc 142(51):21292–21297. https://doi.org/10.1021/jacs.0c11215
73. Ibáñez S, Poyatos M, Dawe LN, Gusev D, Peris E (2016) Ferrocenyl-imidazolylidene ligand for redox-switchable gold-based catalysis. A detailed study on the redox-switching abilities of the ligand. Organometallics 35(16):2747–2758. https://doi.org/10.1021/acs.organomet.6b00517
74. Ibáñez S, Poyatos M, Peris E (2016) A ferrocenyl-benzo-fused imidazolylidene complex of ruthenium as redox-switchable catalyst for the transfer hydrogenation of ketones and imines. ChemCatChem 8(24):3790–3795. https://doi.org/10.1002/cctc.201601025
75. Klenk S, Rupf S, Suntrup L, van der Meer M, Sarkar B (2017) The power of ferrocene, mesoionic carbenes, and gold: redox-switchable catalysis. Organometallics 36(10): 2026–2035. https://doi.org/10.1021/acs.organomet.7b00270
76. Feyrer A, Armbruster MK, Fink K, Breher F (2017) Metal complexes of a redox-active [1] phosphaferrocenophane: structures, electrochemistry and redox-induced catalysis. Chem A Eur J 23(31):7402–7408. https://doi.org/10.1002/chem.201700868
77. Deck E, Wagner HE, Paradies J, Breher F (2019) Redox-responsive phosphonite gold complexes in hydroamination catalysis. Chem Commun 55(37):5323–5326. https://doi.org/10.1039/C9CC01492F
78. Veit P, Volkert C, Förster C, Ksenofontov V, Schlicher S, Bauer M, Heinze K (2019) Gold (II) in redox-switchable gold(I) catalysis. Chem Commun 55(32):4615–4618. https://doi.org/10.1039/C9CC00283A
79. Kita MR, Miller AJM (2014) Cation-modulated reactivity of iridium hydride pincer-crown ether complexes. J Am Chem Soc 136(41):14519–14529. https://doi.org/10.1021/ja507324s
80. Kita MR, Miller AJM (2017) An ion-responsive pincer-crown ether catalyst system for rapid and switchable olefin isomerization. Angew Chem Int Ed 56(20):5498–5502. https://doi.org/10.1002/anie.201701006
81. Gregor LC, Grajeda J, Kita MR, White PS, Vetter AJ, Miller AJM (2016) Modulating the elementary steps of methanol carbonylation by bridging the primary and secondary coordination spheres. Organometallics 35(17):3074–3086. https://doi.org/10.1021/acs.organomet.6b00607
82. Gregor LC, Grajeda J, White PS, Vetter AJ, Miller AJM (2018) Salt-promoted catalytic methanol carbonylation using iridium pincer-crown ether complexes. Cat Sci Technol 8(12): 3133–3143. https://doi.org/10.1039/C8CY00328A